

Complex heavy ion optical potential and the proximity concept

R. Sartor and Fl. Stancu

Institut de Physique B5, Université de Liège, Sart Tilman,
B-4000 Liège 1, Belgium

(Received 6 May 1983)

We show that within the proximity frame and for low bombarding energies, one can construct a complex universal function giving access to both the real and imaginary volume contributions to the heavy ion optical potential.

[NUCLEAR REACTIONS Complex heavy ion optical potential, proximity approximation.]

In order to study the heavy ion optical potential, it is convenient¹⁻⁷ to consider that locally a heavy ion collision can be pictured as that of two nuclear matter systems. Such a model yields the volume contribution (see Ref. 8 for a full discussion) to both the real and imaginary parts of the optical potential. Indeed, in the momentum space, the Fermi sea of the system will be composed of two spheres separated by the relative momentum per nucleon K_r . Such a deformed shape allows for energy conserving collisions and hence for the appearance of the absorptive part in the optical potential. The ambiguities in the exact shape of the two-sphere Fermi sea can be minimized³ by the fact that the radii of the spheres can be determined from the local values of the matter and intrinsic kinetic energy densities ρ and $\tau^{(2)}$, which are thus looked at as the relevant physical quantities in the heavy ion collision. In Ref. 5 one has shown how a complex effective force $v_{ij}^c(r, K_r, \rho, \tau^{(2)})$ could be extracted from the model in order to take into account finite range effects which would otherwise be missed in a purely local application of the model. The optical potential at separation distance D could then be computed⁷ by means of the formula

$$V_{opt}(D) = \langle \Psi(D) | H^c | \Psi(D) \rangle - \langle \Psi(\infty) | H^c | \Psi(\infty) \rangle, \quad (1)$$

with the effective Hamiltonian H^c given by

$$H^c = \sum_i t_i + \frac{1}{2} \sum_{i \neq j} v_{ij}^c(r, K_r, \rho, \tau^{(2)}) . \quad (2)$$

In Ref. 7 $\Psi(D)$ was identified with a totally antisymmetrized two-center harmonic oscillator wave function,^{9,10} and a computation was performed with no further approximation for the ¹⁶O + ¹⁶O system.

In this Brief Report we want to discuss the simplifications brought about by the application of the proximity concept in the computation of V_{opt} . In the proximity frame, the real part of V_{opt} can be written as¹¹

$$\text{Re } V_{opt}(D) = 2\pi \frac{R_1 R_2}{R_1 + R_2} \Phi^R(s); \quad s = D - R_1 - R_2, \quad (3)$$

where R_i is the central radius of nucleus i and $\Phi^R(s)$ is a universal (i.e., ion independent) function defined by

$$\Phi^R(s) = \int_s^\infty e(s') ds', \quad (4)$$

with $e(s')$ denoting the interaction energy per unit surface of two semi-infinite slabs separated by the distance s' .

Corrections for finite curvature¹² and energy dependence¹³ have also been discussed.

Since Eq. (1) yields both the real and imaginary parts V_{opt} , it is interesting to investigate whether relations analogous to (3) and (4) remain valid for $\text{Im } V_{opt}$. The present work should therefore be considered as a practical investigation of the applicability of the proximity concept to the imaginary part of the optical potential. The imaginary contribution to V_{opt} we consider here results from two-body collisions allowed by the Pauli principle. Hence we view the present extension of the proximity concept as complementary to that studied by Randrup and Swiatecki¹⁴ for one-body friction.

The calculation of the complex interaction energy per unit area

$$e^c(s) = e^R(s') + ie^I(s')$$

is based on the energy functional of Refs. 15 and 16. As a prerequisite we have to define the matter distribution of a semi-infinite slab. Following Ref. 17, we assume a distribution of the Fermi type which, by taking the z axis perpendicular to the slab surface, reads

$$\rho(z) = \frac{\rho_0}{1 + e^{z/a}}, \quad (5)$$

where $\rho_0 = 0.17 \text{ fm}^{-3}$ is the saturation density of nuclear matter. The diffuseness a is obtained by minimizing the surface energy of the slab:

$$E_S = 4\pi r_0^2 A^{2/3} \int (H - H_0 \rho) dz; \quad r_0 = \left(\frac{3}{4\pi \rho_0} \right)^{1/3}. \quad (6)$$

In this equation H_0 is the energy density of nuclear matter at saturation and H is the energy density at point z . These quantities have been computed by using the real part of the energy density with the $K_r = 0$ Skyrme parameter set derived in Ref. 16 from Reid soft core G -matrix elements. By using the Thomas-Fermi approximation for the kinetic energy density, one obtains that $a = 0.52 \text{ fm}$ or equivalently¹¹ $b = 0.943 \text{ fm}$ minimizes the integral (6) to $E_S = 26.29 A^{2/3} \text{ MeV}$. This gives a surface energy coefficient $\gamma = 1.668 \text{ MeV fm}^{-2}$.

By using again the complex Skyrme energy densities $H^c(K_r, z)$ obtained in Refs. 15 and 16 we can now define

$e^c(s')$ for two interacting slabs through the usual relation

$$e^c(s') = \int [H^c(K_r, z, 1+2) - H^c(K_r, z, 1) - H^c(K_r, z, 2)] dz, \quad (7)$$

where the extra argument 1+2, 1 and 2 refer to the combined system and to the individual slabs 1 and 2, respectively. We note that $H^c(1)$ and $H^c(2)$ are, in fact, real quantities.¹⁵ In order to calculate $H^c(K_r, z, 1+2)$ we have used the frozen density approximation^{11,18}

$$\rho(z) = \rho_1(z) + \rho_2(z), \quad (8)$$

and the following approximation for the intrinsic kinetic energy density:

$$\tau^{(2)}(z) = \tau_{TF}[\rho(z)] + \frac{K_r^2 \rho_1(z) \rho_2(z)}{\rho(z)}, \quad (9)$$

where $\rho_i(z)$ is the matter density at point z in slab i ($i=1,2$) and $\tau_{TF}[\rho(z)]$ is the Thomas-Fermi approximation to the kinetic energy density corresponding to density ρ . The approximation (9) has been found¹⁹ to be valid at small K_r . The real and imaginary parts of the corresponding universal function (7) are displayed in Figs. 1 and 2, respectively. In Fig. 1 we also show the corresponding universal function ϕ of Ref. 11 to be compared with our result for e^R at $K_r=0$. All functions are given in units of 2γ and are plotted against s in units of b . Although our values of γ and b are different from those of Ref. 11, ϕ and e^R at $K_r=0$ are quite close to each other. This suggests similarities between the basic effective interactions used in each case. Our result for e^R reaches a minimum at $s=0$ because of the Fermi type profile, while in Ref. 11 the density profile obtained from Thomas-Fermi calculations gives a minimum at $s \neq 0$. As far as the energy dependence is concerned we notice only a small difference between the curve at $K_r=0$ and those at $K_r \neq 0$. This can be explained in the following way. The approximation (9) for the intrinsic kinetic energy $\tau^{(2)}$ makes the total kinetic energy density $\tau = \tau^{(2)} + j^2/\rho$ independent of K_r if the current density j is

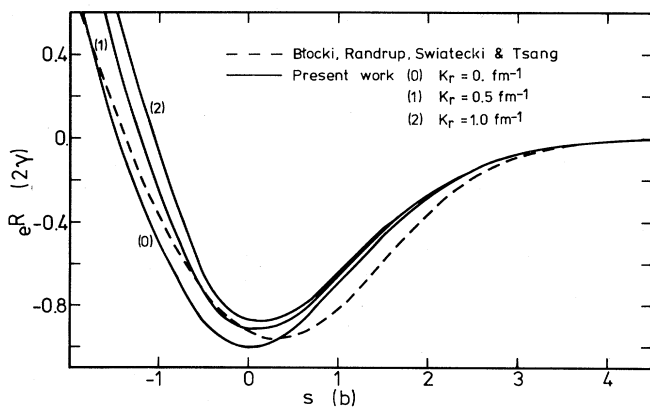


FIG. 1. The real part e^R of the universal function e^c of Eq. (7) (in units of 2γ) as a function of the separation distance s (in units of b) for two interacting slabs. The full curves (0), (1), and (2) represent our result at $K_r=0.0, 0.5$, and 1.0 fm^{-1} , respectively, and the dashed curve comes from Ref. 11.

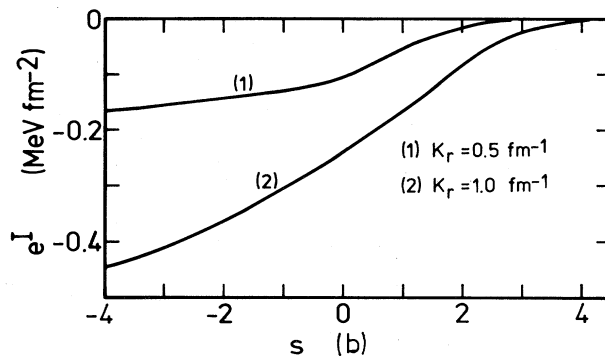


FIG. 2. The imaginary part e^I of the universal function e^c of Eq. (7) as a function of the separation distance s (in units of b) for $K_r=0.5 \text{ fm}^{-1}$ [curve (1)] and $K_r=1.0 \text{ fm}^{-1}$ [curve (2)].

treated in the approximation $j \simeq (K_r/2)(\rho_1 - \rho_2)$ as shown in Ref. 19. Hence, at $K_r \neq 0$, the energy dependence should entirely come from the potential part H_{pot} of $\text{Re}H^c$:

$$H_{\text{pot}} = \frac{3}{8} t_0 \rho^2 + \frac{1}{16} t_3 \rho^3 + \frac{1}{16} (3t_1 + 5t_2) \rho \tau^{(2)} + \frac{1}{64} (9t_1 - 5t_2) (\nabla \rho)^2. \quad (10)$$

It occurs, however, that the energy dependence contained¹⁶ in the Skyrme parameters t_i ($i=0-2$) is counteracted to a large extent by the energy dependence of $\tau^{(2)}$ as given by Eq. (9). Such a compensation effect is consistent with the results of Ref. 7 (see Fig. 3).

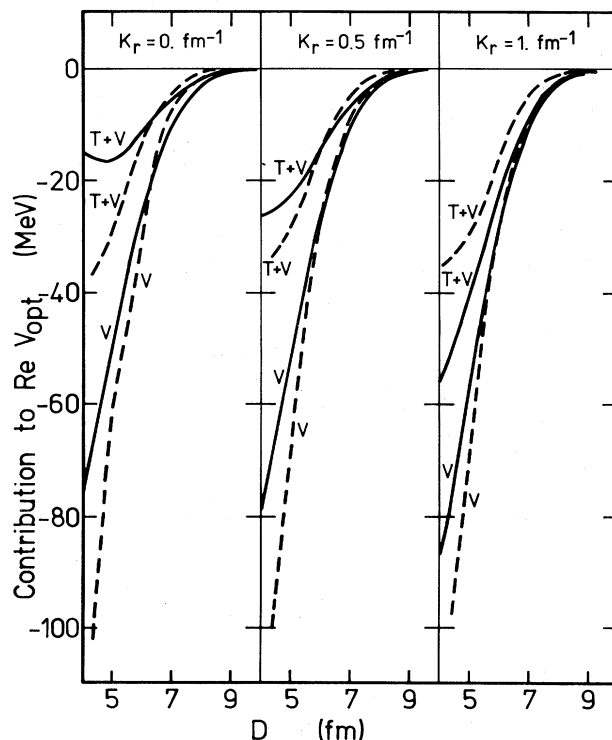


FIG. 3. The real part $T+V$ of the optical potential for $^{16}\text{O}+^{16}\text{O}$ as a function of D at three different relative momenta. Full curve: present result; dashed curve: Ref. 7. We also indicate the potential part V only in each case.

In its complex form the potential part of the energy functional H^c is^{15,16}

$$H_{\text{pot}}^c = [1 + i\xi(\rho, \tau^{(2)})]H_{\text{pot}}, \quad (11)$$

where $\xi(\rho, \tau^{(2)})$ is a scaling factor defined in Ref. 15 which depends on the local values of ρ and $\tau^{(2)}$. The imaginary proximity function e^I calculated from Eqs. (7) and (11) and plotted in Fig. 2 shows a very pronounced energy dependence. According to the above discussion for e^R the energy dependence of e^I comes essentially from ξ which depends on energy through $\tau^{(2)}$.

The universal functions of Figs. 1 and 2 have been used to calculate the complex proximity potential for $^{16}\text{O} + ^{16}\text{O}$ and the result is shown in Figs. 3 and 4. This pair has been chosen in order to compare the proximity potential with what we call the "exact" results of Ref. 7, also indicated in Figs. 3 and 4. In Eq. (3) we took $R_f = 2.7$ fm, which is the value of the rms radius obtained with a harmonic oscillator shell model for ^{16}O with a size parameter equal to 1.8 fm as used in Ref. 7.

In Fig. 3, $\text{Re}V_{\text{opt}}$ corresponds to the curves called $T + V$, i.e., contain the contribution from both the kinetic and potential parts of $\text{Re}H^c$. In order to see to what extent the approximation for τ is responsible for the disagreement with the calculations of Ref. 7, we have also separately drawn the potential part contribution called V . For all values of K_r at large separation distances there is a good agreement between the present results and those of Ref. 7. Less good is the agreement for $T + V$, and this is essentially due to the approximation for τ implied by Eq. (9).

In Fig. 4 the comparison is made for $\text{Im}V_{\text{opt}}$. It can be seen that in the physically relevant tail region, the proximity approach leads to fairly good results at low bombarding energies ($K_r \leq 0.5 \text{ fm}^{-1}$). The discrepancies for small separation distances or for higher energies ($K_r = 1 \text{ fm}^{-1}$) are to be ascribed to the deficiencies in approximations (8) and (9). In particular, the frozen density approximation (8) does not take antisymmetrization effects into account while, as discussed in Ref. 19, approximation (9) overestimates $\tau^{(2)}$. This enhances the corresponding deformation of the local Fermi sea and hence leads to too strong an absorption.

The present results show, however, that the proximity re-

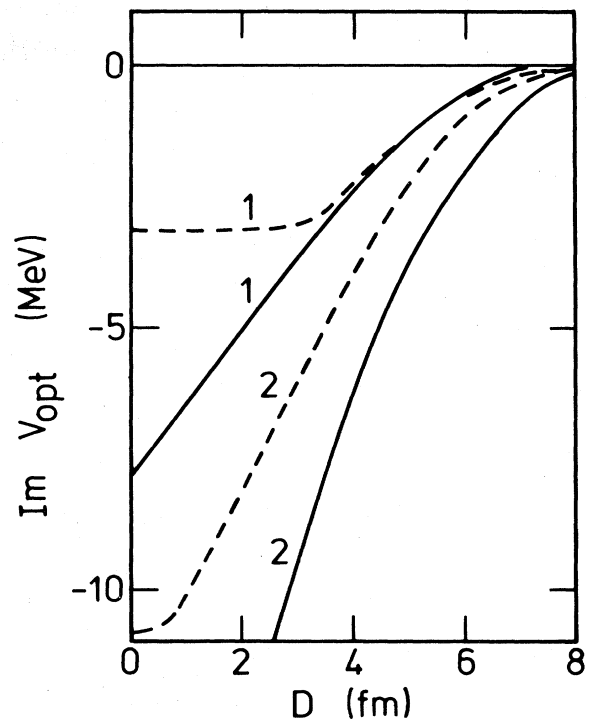


FIG. 4. $\text{Im}V_{\text{opt}}$ for $^{16}\text{O} + ^{16}\text{O}$ as a function of D at $K_r = 0.5 \text{ fm}^{-1}$ (curve 1) and $K_r = 1.0 \text{ fm}^{-1}$ (curve 2). Full curves: present results; dashed curves: Ref. 7.

lation (3), together with our universal functions Φ^R and Φ^I , provides a reliable first approximation to the tail region of the low energy heavy ion optical potential. This suggests that the proximity approach can be used as an alternative to more elaborate calculations, not only for the real part but also for the volume contribution to the imaginary part.

One of us (R.S.) thanks the Institut Interuniversitaire des Sciences Nucléaires for financial support.

¹D. A. Saloner and C. Toepffer, Nucl. Phys. **A283**, 108 (1977).

²F. Beck, K. H. Müller, and H. S. Köhler, Phys. Rev. Lett. **40**, 837 (1978).

³T. Izumoto, S. Krewald, and A. Faessler, Nucl. Phys. **A341**, 319 (1980).

⁴E. S. Hernandez and S. A. Moskowsky, Phys. Rev. C **21**, 929 (1980).

⁵A. Faessler, T. Izumoto, S. Krewald, and R. Sartor, Nucl. Phys. **A359**, 509 (1981).

⁶N. J. di Giacomo, J. C. Peng, and R. M. De Vries, Phys. Lett. **101B**, 383 (1981).

⁷R. Sartor, A. Faessler, S. B. Khadkikar, and S. Krewald, Nucl. Phys. **A359**, 467 (1981).

⁸S. B. Khadkikar, L. Rikus, A. Faessler, and R. Sartor, Nucl. Phys. **A369**, 495 (1981).

⁹T. Fliessbach, Z. Phys. A **238**, 329 (1970); **242**, 287 (1971); **247**, 117 (1971).

¹⁰D. M. Brink and Fl. Stancu, Nucl. Phys. **A243**, 175 (1975).

¹¹J. Błocki, J. Randrup, W. J. Swiatecki, and C. F. Tang, Ann. Phys. (N.Y.) **105**, 427 (1977).

¹²D. M. Brink and Fl. Stancu, Nucl. Phys. **A299**, 321 (1978).

¹³S. A. Moszkowski, Nucl. Phys. **A309**, 273 (1978).

¹⁴J. Randrup and W. J. Swiatecki, Ann. Phys. (N.Y.) **125**, 193 (1980).

¹⁵R. Sartor and Fl. Stancu, Phys. Rev. C **24**, 2347 (1981).

¹⁶R. Sartor and Fl. Stancu, Nucl. Phys. (in press).

¹⁷S. A. Moszkowski, Phys. Rev. C **2**, 402 (1970).

¹⁸K. A. Brueckner, J. R. Buchler, and M. M. Kelly, Phys. Rev. **173**, 944 (1968).

¹⁹R. Sartor and A. Faessler, Nucl. Phys. **A376**, 263 (1982).